Electronic Supplementary Material (ESI) for Physical Chemistry Chemical Physics.

Supporting Information: Insight the Active role of Excess Hydroxyl ion in Silicate Condensation Reaction

Tuong Ha Do,[†] Hien Duy Tong,[‡] Khanh-Quang Tran,[¶] Evert Jan Meijer,[*,§] and Thuat T. Trinh[*,‖]

†Faculty of Applied Sciences, Ton Duc Thang University, 19 Nguyen Huu Tho, Tan Phong ward, District 7, Ho Chi Minh City, Vietnam, E-mail:dotuongha@tdtu.edu.vn

‡Faculty of Engineering, Vietnamese-German University (VGU), Thu Dau Mot City, Binh Duong Province, Vietnam

¶Department of Energy and Process Engineering, Norwegian University of Science and Technology, Kolbjørn Hejes vei 1B, Trondheim, Norway

§Van't Hoff Institute for Molecular Sciences, University of Amsterdam, Amsterdam, The Netherlands

‖Department of Chemistry, Norwegian University of Science and Technology, Høgskoleringen 5, 7491-Trondheim, Norway

E-mail: e.j.meijer@uva.nl; thuat.trinh@ntnu.no

Thermodynamic integration method

As mentioned in the main text that the free energy (ΔG) profiles of the oligomerization reactions were obtained by thermodynamic integration using eq.1

$$\Delta G = \int_{r_1}^{r_2} \langle F(r) \rangle \, dr \tag{1}$$

We calculated the constraint force (F) at a fixed value of the reaction coordinate (r) to investigate the free energy profiles of condensation reactions. The integral limits (r_1 and r_2) were obtained from the unconstrained AIMD simulations where the forces were typically zero. We provided an example of three different condensation reactions (trimer, 3-ring, and 4-ring) in Table S1. To obtain the free energy profiles, we plotted the integral for each reaction step with the reactant state as the reference, as shown in Fig S1. In the first reaction step, the two silicate molecules were far apart in the reactant state and formed a Si-OSi bond in the product state. As the reaction proceeded, the distance between the two molecules decreased ($r_1 > r_2$). Therefore, the value of r_1 was larger than r_2 in the first step. Conversely, in the second reaction step, the reactant state was at the Si-O bonding state, and the product state was when the Si...O distance was far away. As the reaction proceeded, the distance between the two molecules increased ($r_1 < r_2$).

Table S1: Example of integration limits of the reaction coordinate r_1, r_2 obtained by unconstrained AIMD simulations.

Formation of silicate	Reaction step	r_1 (Å)	r_2 (Å)
Trimer	First step	3.77	1.84
	Second step	1.74	3.82
3-ring	First step	3.79	1.78
	Second step	1.81	3.77
4-ring	First step	3.75	1.77
	Second step	1.77	3.72

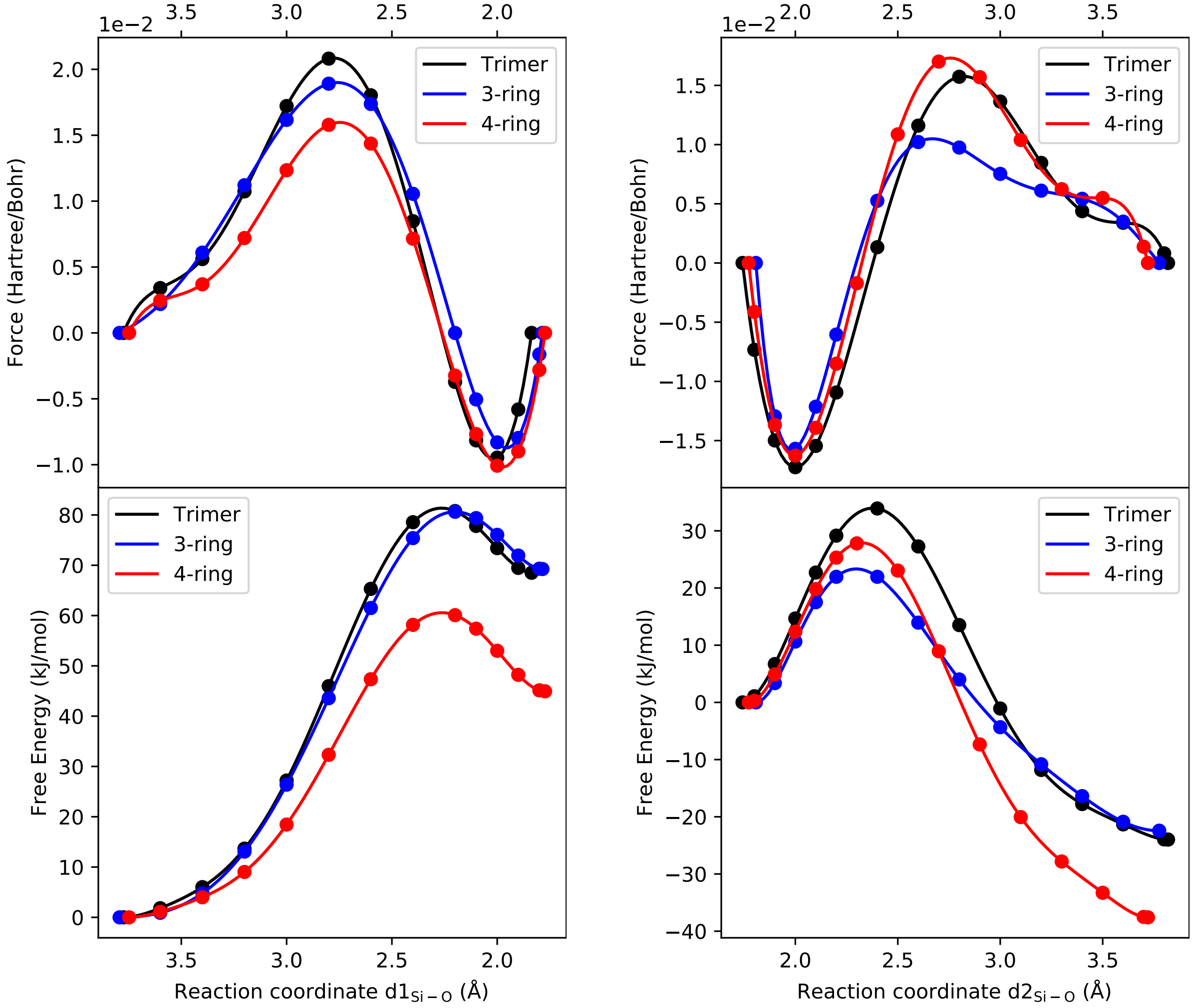

(a) First reaction step

(b) Second reaction step

Figure S1: Mean force of constraint, free energy values vs the reaction coordinates for selected reactions for form trimer, 3-ring and 4-ring obtained with AIMD simulations using CP2K. See the main text for more details.

Radial distribution function of water

The radial distribution function of Ow-Ow and Ow-Hw was calculated with AIMD and plotted in Fig S2. As described in the main text, we employed PBE with Grimme D2[S1] correction for dispersion interaction. To compare with literature, we also adopted the calculation from SCAN functional and experimental data from SCAN functional[S2] and experimental results[S3,S4] is presented.

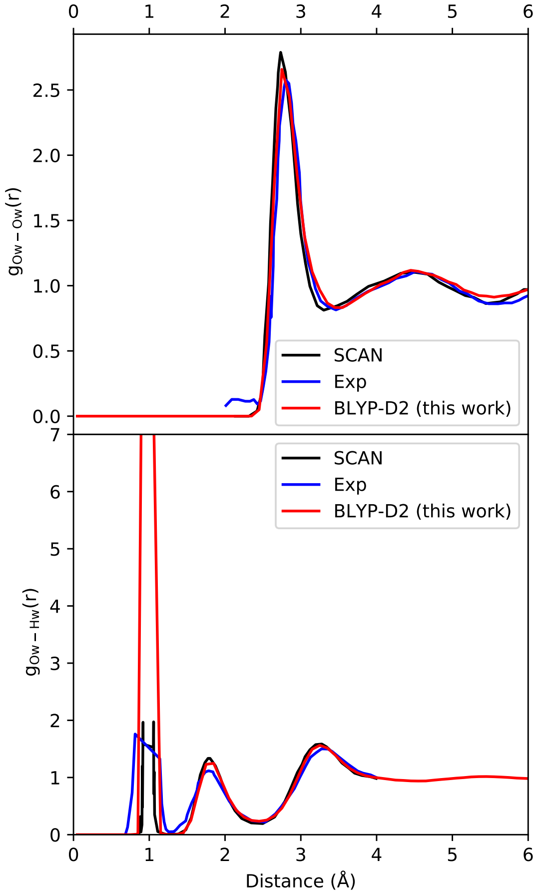

Figure S2: Radial distribution function of Ow-Ow and Ow-Hw of water calculated with AIMD using BLYP-D2 functional. RDFs profiles obtained from SCAN functional and experimental data are also included for comparison. Excellent agreement between these methods is shown.

Molecular orbital of silicate structures

Structure	HOMO	LUMO
Dimer	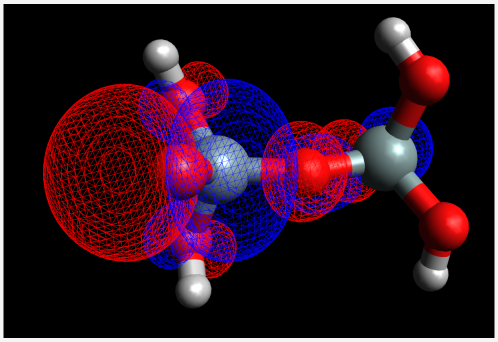	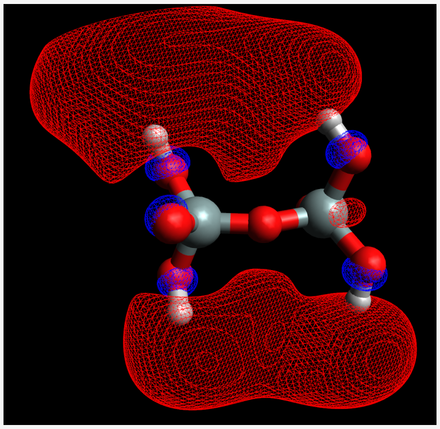
Trimer	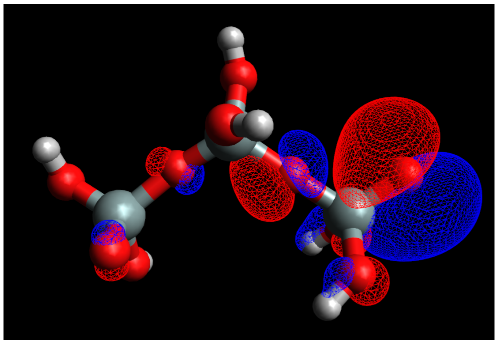	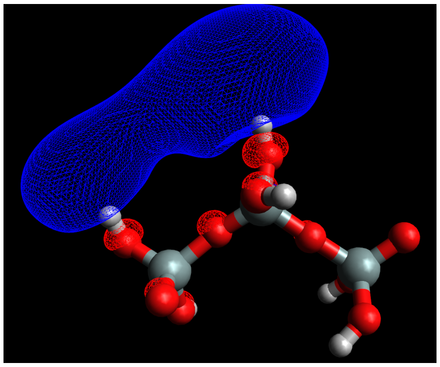
3-ring	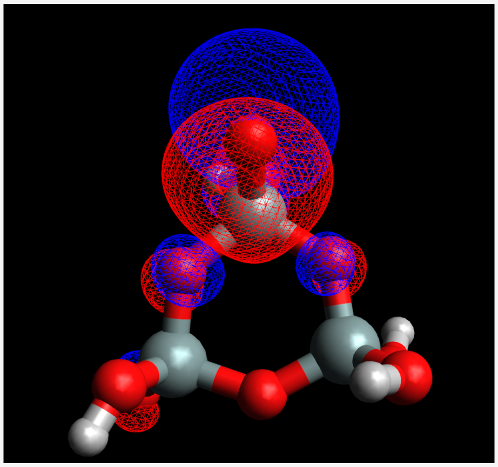	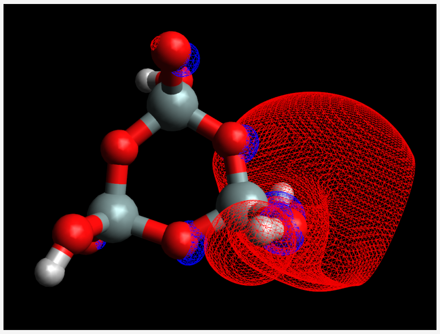

Figure S3: HOMO and LUMO orbitals of the silicate product of dimer, trimer and 3-ring species

Structure	HOMO	LUMO
Linear tetramer	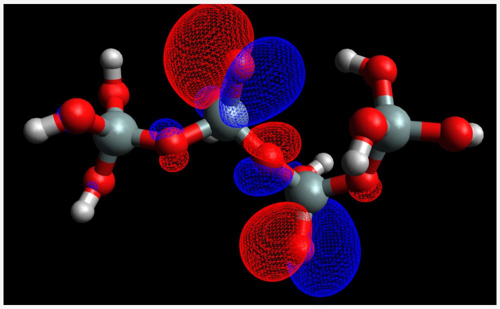	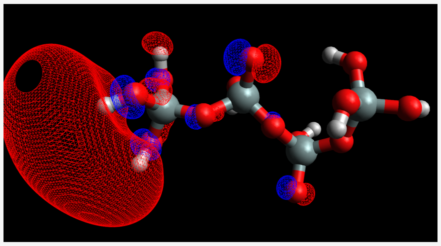
Branched tetramer	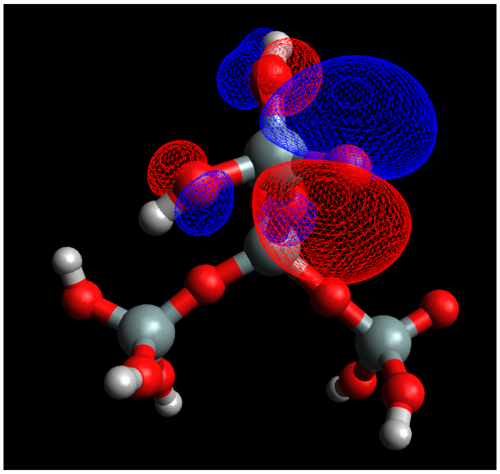	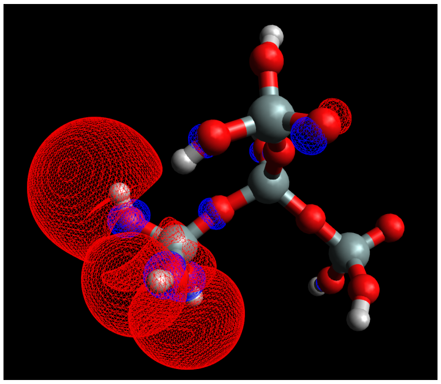
4-ring	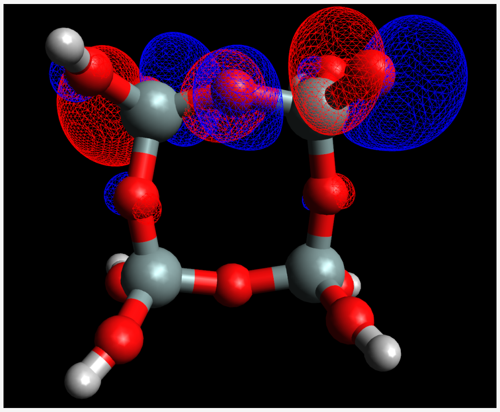	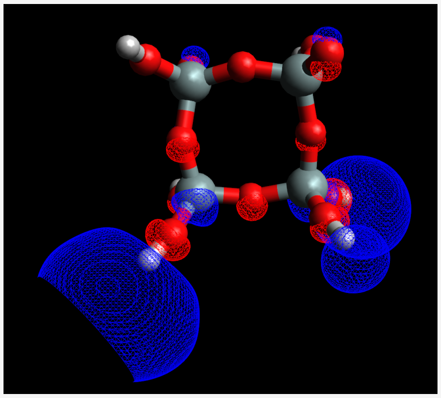

Figure S4: HOMO and LUMO orbitals of the silicate product of linear tetramer, branched tetramer and 4-ring species

An illustration of highest occupied molecular orbital (HOMO) and lowest unoccupied molecular orbital (LUMO) of all six silicate structures studied in this work.

Bonds and angles of 3-ring and 4-ring structures

The bonds and angles in the 3-ring and 4-ring structures obtained by AIMD simulations. See the main text for more details.

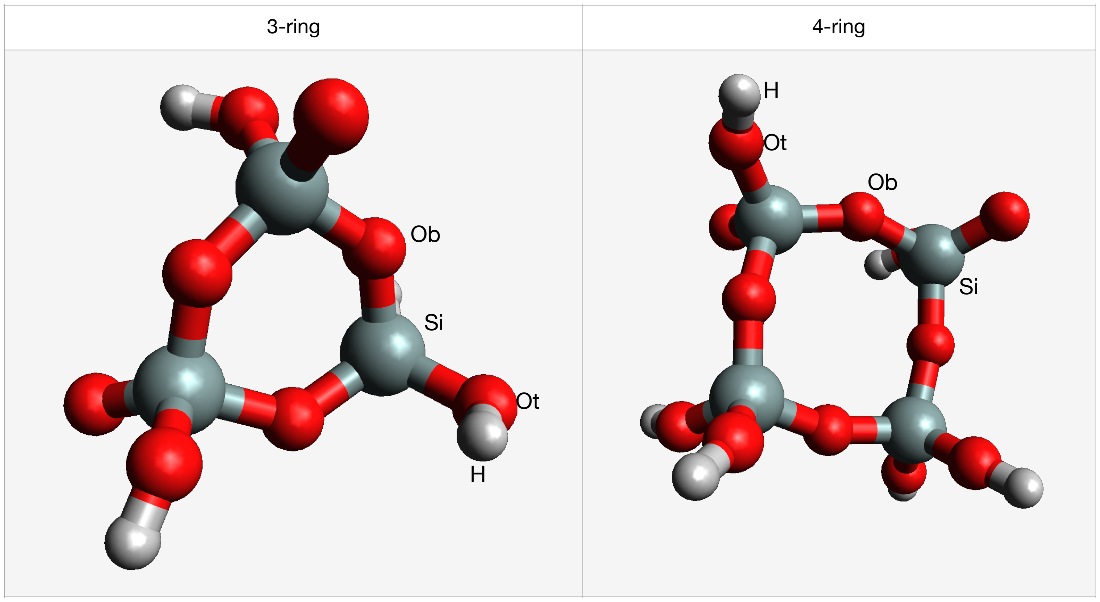

Figure S5: Structure of 3-ring and 4-ring product species during AIMD simulations. The water molecules around the silicate was removed for a better visualization. For a comparison with previous DFT calculations, selected bond lengths and angles were calculated and presented in Table S2

Table S2: Selected bond lengths and angles of the 3-ring and 4-ring silicate products obtained by AIMD simulations. The silicate structure is depicted in Fig S5. The minimums and maximums are calculated to compare with previous static DFT calculations.[S5] The last column presents the average values during the last 10ps run of AIMD.

	3-ring	Static DFT^a	AIMD (this work)	AIMD average (this work)
distance (Å)	O-H	0.99 - 1.10	0.937 - 1.140	1.003 ± 0.038
distance (Å)	Si-Ot	1.65 - 1.68	1.546 - 1.744	1.652 ± 0.044
distance (Å)	Si-Ob	1.69 - 1.70	1.546 - 1.753	1.659 ± 0.044
angle (°)	ObSiOb	102.2 - 103.9	98.126 - 116.647	108.144 ± 4.980
angle (°)	OtSiOt	110.7 - 116.4	95.720 - 123.083	108.146 ± 4.361
angle (°)	SiOH	110.9 - 128.8	103.302 - 132.836	116.329 ± 6.731
	4-ring	Static DFT^b		
distance (Å)	O-H	0.99 - 1.08	0.914 - 1.096	0.988 ± 0.032
distance (Å)	Si-Ot	1.64 - 1.71	1.553 - 1.729	1.646 ± 0.039
distance (Å)	Si-Ob	1.64 - 1.70	1.530 - 1.811	1.649 ± 0.049
angle (°)	ObSiOb	104.9 - 108.8	93.509 - 118.443	106.810 ± 6.551
angle (°)	OtSiOt	108.4 - 116.3	93.509 - 125.359	109.435 ± 5.476
angle (°)	SiOH	117.6 - 124.8	95.081 - 179.668	124.032 ± 17.514

^{a} using 16 water molecules; ^{b} using 18 water molecules.

References

(S1) Grimme, S. Semiempirical GGA-type density functional constructed with a long-range dispersion correction. *J. Comput. Chem.* **2006**, *27*, 1787–1799.

(S2) Chen, M.; Ko, H.-Y.; Remsing, R. C.; Calegari Andrade, M. F.; Santra, B.; Sun, Z.; Selloni, A.; Car, R.; Klein, M. L.; Perdew, J. P.; Wu, X. Ab initio theory and modeling of water. *Proc. Natl. Acad. Sci. U.S.A.* **2017**, *114*, 10846–10851.

(S3) Soper, A.; Benmore, C. Quantum Differences between Heavy and Light Water. *Phys. Rev. Lett.* **2008**, *101*, 065502.

(S4) Skinner, L. B.; Huang, C.; Schlesinger, D.; Pettersson, L. G.; Nilsson, A.; Benmore, C. J. Benchmark oxygen-oxygen pair-distribution function of ambient water from x-ray diffraction measurements with a wide ¡i¿Q¡/i¿-range. *The Journal of Chemical Physics* **2013**, *138*, 074506.

(S5) Schaffer, C. L.; Thomson, K. T. Density Functional Theory Investigation into Structure and Reactivity of Prenucleation Silica Species. *J. Phys. Chem. C* **2008**, *112*, 12653–12662.